Implementation of the Coupled Ocean-Atmosphere Response Experiment flux algorithm with CO_2, dimethyl sulfide, and O_3

C. W. Fairall,[1] Mingxi Yang,[2] Ludovic Bariteau,[3] J. B. Edson,[4] D. Helmig,[5] W. McGillis,[6] S. Pezoa,[1] J. E. Hare,[3,7] B. Huebert,[2] and B. Blomquist[2]

Received 13 December 2010; revised 15 July 2011; accepted 3 August 2011; published 27 October 2011.

[1] Updates for the Coupled Ocean-Atmosphere Response Experiment (COARE) physically based meteorological and gas transfer bulk flux algorithms are examined. The current versions are summarized and a generalization of the gas transfer codes to 79 gases is described. The current meteorological version COARE3.0 was compared with a collection of 26,700 covariance observations of drag and heat transfer coefficients (compiled from three independent research groups). The algorithm agreed on average to within 5% with observations for a wind speed range of 2 to 18 m s^{-1}. Covariance observations of CO_2 and dimethyl sulfide (DMS) gas transfer velocity k were normalized to Schmidt number 660 and compared to an ensemble of gas flux observations from six research groups and nine field programs. A reasonable fit of the mean k_{660} versus U_{10n} values was obtained for both CO_2 and DMS with a new version of the COARE gas transfer algorithm (designated COAREG3.1) using friction velocity associated with viscous (tangential) stress, $u_{*\nu}$, in the nonbubble term. In the wind speed range 5 to 16 m s^{-1}, tracer-derived estimates of k_{660} are 10% to 20% lower than the CO_2 covariance estimates presented here.

Citation: Fairall, C. W., M. Yang, L. Bariteau, J. B. Edson, D. Helmig, W. McGillis, S. Pezoa, J. E. Hare, B. Huebert, and B. Blomquist (2011), Implementation of the Coupled Ocean-Atmosphere Response Experiment flux algorithm with CO_2, dimethyl sulfide, and O_3, *J. Geophys. Res.*, *116*, C00F09, doi:10.1029/2010JC006884.

1. Introduction

[2] Parameterizations of air-sea transfer of trace gases center on characterization of the transfer velocity, k, which may be partitioned into waterside (k_w) and airside (k_a) components. While accurate k parameterization is only one aspect of global chemical flux issues (e.g., *Signorini and McClain* [2009] discuss the relative uncertainties in CO_2 flux estimates associated with uncertainties in wind speed, oceanic gas concentrations, and k algorithms), it plays an important role in ocean and atmospheric modeling, global chemical budgets, and the ocean observing system [*Fairall et al.*, 2010]. Historically, k is represented with simple power laws in wind speed at 10 m above the ocean surface, U_{10}. Based on lake measurements of SF_6 and wind tunnel observations, *Liss and Merlivat* [1986] modeled k_w as three piecewise linear functions of wind speed with increasing slope toward higher winds. Based on natural ^{14}C disequilibrium and the bomb ^{14}C inventory, *Wanninkhof* [1992, hereinafter W92] fitted a quadratic relationship between k and ship-based U_{10}. From artificial injections of two volatile tracers (^3He and SF_6) and a nonvolatile tracer (spores) in the North Sea, *Nightingale et al.* [2000] parameterized k with both a linear and a quadratic term with respect to U_{10}. Advancements in sensor technologies led to the application of the micrometeorological direct covariance method to estimate fluxes at hourly time scales on the atmospheric side of the interface. This method was first successfully applied in the so-called Gas Exchange (GasEx) field programs beginning in 1998 [*Fairall et al.*, 2000].

[3] The short time scale of the covariance estimates enables observational investigations of the relationship of k to physical/chemical forcing beyond wind speed. Examples include wind stress, buoyancy flux, surfactants, or surface gravity wave properties. This is critical because theoretical advances [e.g., *Soloviev and Schlüssel*, 1994] have outstripped observations. In other words, gas transfer parameterization has faced a substantial data gap. Physically based parameterizations [*Hare et al.*, 2004; *Soloviev*, 2007; *Vlahos and Monahan*, 2009] are now available that incorporate these additional forcing factors and may lead to quite different transfer properties for different gases. For example, the dependence of bubble-mediated exchange on gas solubility implies the *W92* formula may not be appropriate for the fairly soluble biogenic sulfur gas dimethyl sulfide (DMS) [*Woolf*, 1993; *Blomquist et al.*, 2006]. Thus, application of a single wind speed formula for all gases is inconsistent with

[1]NOAA Earth System Research Laboratory, Boulder, Colorado, USA.
[2]Department of Oceanography, University of Hawaii, Honolulu, Hawaii, USA.
[3]Cooperative Institute for Research in Environmental Sciences, University of Colorado at Boulder, Boulder, Colorado, USA.
[4]Department of Marine Sciences, University of Connecticut, Groton, Connecticut, USA.
[5]Institute of Alpine and Arctic Research, University of Colorado at Boulder, Boulder, Colorado, USA.
[6]Lamont-Doherty Earth Observatory, Columbia University, Palisades, New York, USA.
[7]Now at Joint Institute for Marine and Atmospheric Research, University of Hawai'i at Mānoa, Honolulu, Hawaii, USA.

0148-0227/11/2010JC006884

Table 1. History of the COARE Algorithms[a]

Year	Algorithm	Reference
1996	COARE2.5	*Fairall et al.* [1996a, 1996b]
2000	COAREG2.5_CO_2	*Fairall et al.* [2000] and *Hare et al.* [2004]
2003	COARE3.0	*Fairall et al.* [2003]
2004	COAREG3.0_DMS	*Blomquist et al.* [2006]
2006	COAREG3.0_Ozone	*Fairall et al.* [2007]
2008	PCBs, PCDEs	*Perlinger and Rowe* [2008]
2010	79 Gases	*Johnson* [2010] and *Rowe et al.* [2011]
2011	COAREG3.1 CO_2, DMS, Ozone, SF_6, ^3He	This study

[a]The terminology COARE*N.M* refers to publically available versions of the meteorological flux algorithm.

current understanding of gas transfer physics. For an excellent summary of gas transfer observation methods and the current state-of-the-art in parameterizations, see *Wanninkhof et al.* [2009].

[4] In this paper we focus on updating one of the physically based parameterizations, the Coupled Ocean-Atmosphere Response Experiment (COARE) family of gas transfer algorithms. The terminology COARE is a legacy from the original field program [*Webster and Lukas*, 1992] that pioneered the meteorological algorithm. Our goal here is to synthesize recent theoretical advances and results from field programs of the last decade. Following a description of the algorithms (section 2), we discuss theoretical issues associated with wave effects and the partition of total wind stress at the surface into tangential (viscous) and gravity wave (pressure) components (section 3). In section 4 we give the results for meteorological fluxes, selected gas fluxes, and also attempt to rationalize the adjustable parameters in a new version of the COARE gas transfer algorithm (designated COAREG3.1) for CO_2 and DMS. Conclusions are given in section 5.

2. Background on COARE Family of Parameterizations

2.1. History

[5] The international COARE field program took place in the western Pacific warm pool over 4 months from November 1992 to February 1993. Development of a bulk air-sea flux algorithm for use by the COARE community began almost immediately. Version COARE2.0 (released August 1994) included code to model the ocean cool skin physics and also daytime near-surface warming based on a simplified version of the *Price et al.* [1986] ocean mixing model [*Fairall et al.*, 1996a]. A major modification to the algorithm was made at a the Third Workshop of the Tropical Ocean–Global Atmosphere (TOGA) COARE Air-Sea Interaction (Flux) Working Group (University Corporation for Atmospheric Research/TOGA COARE International Project Office, Honolulu, Hawaii, 2–4 August 1995). Transfer coefficients were reduced by six percent to give better average agreement with covariance latent heat fluxes from several COARE ships. The version COARE2.5b bulk algorithm was released [*Fairall et al.*, 1996b], consisting of both the FORTRAN and MATLAB source codes, a test data set, and the corresponding computed flux results. Version 2.5b had been developed using COARE measurements exclusively, which were limited to wind speeds in the range 0–12 m s^{-1} and the tropical environment. *Fairall et al.* [2003] released version COARE3.0 which added data from multiple nonequatorial field programs, made adjustments to the drag and scalar transfer coefficients at higher wind speeds, and added two, user-selectable, wave state–dependent formulations for the Charnock parameter.

[6] A CO_2 transfer velocity parameterization was originally developed as an extension of the COARE cool skin model adapting the work of *Soloviev and Schlüssel* [1994]. Details are given by *Fairall et al.* [2000] and *Hare et al.* [2004]. Subsequent extensions to other gases are given in Table 1.

2.2. Current Version for Meteorological Fluxes

[7] The turbulent stress vector components on the ocean are represented as

$$\tau_x = \rho_a C_{dz} S U_x, \tag{1a}$$

$$\tau_y = \rho_a C_{dz} S U_y, \tag{1b}$$

where ρ_a is the density of air, S is the wind speed, U_x and U_y are the vector-averaged wind components (all specified at height above the surface z and relative to the sea surface which accounts for surface current) and C_{dz} the stability-dependent drag coefficient at z. Note that in this form the stress and wind vectors are aligned. Thus, if the coordinate system is rotated to align the x axis with the mean wind vector, then the streamwise stress is

$$\tau = \rho_a C_{dz} S \left[(U_x)^2 + (U_y)^2 \right]^{1/2} = \rho_a u_*^2, \tag{2}$$

where u_* is the friction velocity and cross-stream stress is zero. COARE makes a distinction between the mean magnitude of the wind vector, $S = \sqrt{\overline{U_x^2 + U_y^2}} = \sqrt{(\overline{U_x})^2 + (\overline{U_y})^2 + U_G^2}$, and the magnitude of the mean vector $U = \sqrt{(\overline{U_x})^2 + (\overline{U_y})^2}$ through the factor U_G that represents the gustiness (wind variability) of the atmospheric boundary layer. Gustiness allows the scalar fluxes to remain nonzero and promotes smooth variation of the scalar transfer coefficients as the mean vector wind approaches zero.

[8] The drag coefficient is related to the velocity roughness length, z_o, by

$$C_{dz} = \frac{\kappa^2}{[\log(z/z_o) - \psi_u(z/L)]^2}, \tag{3}$$

where $\kappa = 0.4$, L is the Monin-Obukhov stability length, and ψ_u the wind profile stability function. It is also common to see z_o expressed as the 10 m neutral drag coefficient

$$C_{d10n} = \frac{\kappa^2}{[\log(10/z_o)]^2}. \tag{4}$$

Specification of z_o is equivalent to expressing the neutral drag coefficient. COARE3.0 specifies z_o as a *Smith* [1988]-type form with the combination of a smooth flow and a Charnock (gravity wave) relation

$$z_o = 0.11\nu/u_* + a_C u_*^2/g. \tag{5}$$

Here a_C is the Charnock coefficient, ν the kinematic viscosity of air, and g the acceleration of gravity. Three different representations of a_C are allowed: (1) a wind speed dependence, (2) a wave-age parameterization from *Oost et al.* [2002], and (3) a wave-slope parameterization from *Taylor and Yelland* [2001].

[9] The sensible and latent heat fluxes from the ocean are represented as

$$H_s = \rho_a c_{pa} C_{Hz} S(\theta_s - \theta_a), \tag{6a}$$

$$H_l = \rho_a L_e C_{Ez} S(q_s - q_a), \tag{6b}$$

where θ is the mean potential temperature at the surface (subscript s) and in the air (subscript a) at reference height z; q the water vapor mixing ratio at the surface (vapor pressure of seawater at the surface temperature) and in the air at reference height z; c_{pa} the specific heat of air, L_e the latent heat of vaporization of water, and C_{Hz}, C_{Ez} the heat transfer coefficients.

[10] The heat transfer coefficients are related to the scalar roughness lengths, z_{ot} and z_{oq}, by

$$C_{Hz} = \frac{\kappa}{[\log(z/z_o) - \psi_u(z/L)]} \frac{\kappa}{[\log(z/z_{ot}) - \psi_h(z/L)]}, \tag{7}$$

where ψ_h is the scalar profile stability function. The 10 m neutral transfer coefficient and scalar roughness lengths are related by

$$C_{H10n} = C_{d10n}^{1/2} \frac{\kappa}{[\log(10/z_{ot})]}. \tag{8}$$

The scalar roughness parameters (z_{ot}, z_{oq}) are obtained using simple relationships to the roughness Reynolds number ($R_r = u_* z_o/\nu$) as

$$z_{oq} = z_{ot} = \min\left(1.15\ 10^{-4}, 5.5\ 10^{-5}\ R_r^{-0.6}\right), \tag{9}$$

which fit the Earth Systems Research Laboratory (ESRL) ship-based flux observations and tower-based observations from the North Sea [*DeCosmo et al.*, 1996; see *Fairall et al.*, 2003, Figure 4]. *Fairall et al.* [2003] found COARE3.0 to be a good fit, on average, to observed momentum and latent heat fluxes over a wind speed range of 0 to 18 m s^{-1}.

2.3. Version 3.0 for Trace Gas Fluxes

[11] The flux of a trace gas on the atmospheric side of the interface is estimated as

$$F_c = \alpha k(C_w/\alpha - C_a) = \alpha k \Delta C = \left[\frac{\alpha k}{u_*}\right] u_* \Delta C = CP_c u_* \Delta C, \tag{10}$$

where k is the transfer velocity, α is dimensionless solubility, C_w and C_a the mean concentration of the gas in the water and air at reference depth and height. In the final term on the RHS of (10) we separate the flux computation into a chemical factor, CP_c, and a physical forcing factor $u_*\Delta$C, which we discuss further in section 2.4. The COARE gas transfer algorithm (generically referred to as COAREG, current public version called COAREG3.0) gives a simple form for the transfer velocity [see *Hare et al.*, 2004]

$$k = \frac{u_*}{r_w + \alpha r_a}, \tag{11}$$

where

$$r_w = \left[r_{wt}^{-1} + k_b/u_*\right]^{-1}. \tag{12}$$

Here u_*/r_{wt} represents molecular-turbulent transfer and k_b represents bubble transfer. On the atmospheric side we neglect spray-mediated gas transfer, so there is only molecular-turbulent transfer $r_a = r_{at.}$

[12] In the COAREG model the individual terms are represented as

$$r_{wt} = [\rho_w/\rho_a]^{1/2}\left[h_w S_{cw}^{1/2} + \kappa^{-1}\ln(z_w/\delta_w)\right], \tag{13}$$

where z_w is the water depth of the reference measurements, δ_w the molecular sublayer thickness, S_{cw} the Schmidt number of water, ρ_w the density of water, and

$$h_w = 13.3/(A\phi). \tag{14}$$

In this expression, A is an empirical constant and ϕ accounts for surface buoyancy flux enhancement of the transfer. A similar expression is used for r_{at}, but the molecular sublayer thickness is explicitly approximated by incorporating the velocity drag coefficient, C_d, which is a function of the atmospheric measurement height, z_a,

$$r_{at} = \left[h_a S_{ca}^{1/2} + C_d^{-1/2}(z_a) - 5 + \ln(S_{ca})/(2\kappa)\right], \tag{15}$$

where h_a = 13.3. The bubble driven part of the transfer is taken from *Woolf* [1997] as

$$k_b = BV_o f_{wh}\alpha^{-1}\left[1 + \left(e\alpha S_{cw}^{-1/2}\right)^{-1/n}\right]^{-n}, \tag{16}$$

where B is a second adjustable constant, V_o = 2450 cm h^{-1}, f_{wh} is the whitecap fraction, e = 14, and n = 1.2 for CO_2 (we use these values for all gases). The parameters A and B have been adjusted to fit observations but so far represent a "moving target" with values between 1.0 and 2.0. The balance of the direct and bubble-mediated transfer is discussed in more detail in Appendix A.

[13] CO_2 transfer velocities observed at some temperature, T, are often expressed in terms of the value they translate to at T = 20°C where S_{cw} = 660 for CO_2

$$k_{660} = k\left[\frac{S_{cw}(T)}{660}\right]^{1/2}. \tag{17}$$

Furthermore, a similar approach is used to estimate gas transfer of one gas from observations of k from another gas. Similarly, observations of transfer velocity of DMS may be

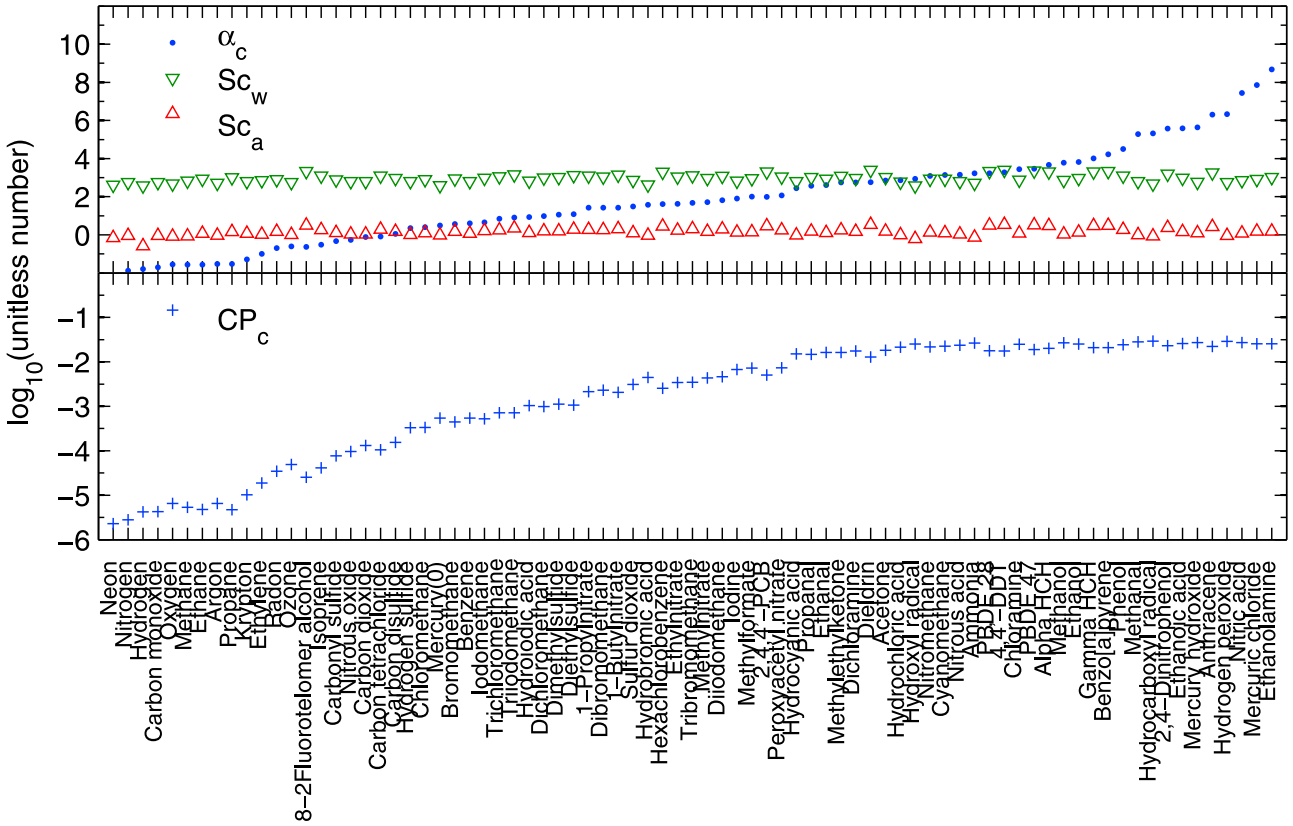

Figure 1. The chemical parameter, CP_c, computed for seawater at near-neutral stability, wind speed $U_{10n} = 11$ m s^{-1}, and $u_* = 0.4$ m s^{-1} for chemicals having a range in solubility at 20°C. For information about values of the other parameters used in computing these CP_c values, see *Rowe et al.* [2011]. Solubility and air- and water-side Schmidt numbers are shown for comparison.

expressed at S_{c_DMS} = 660 for comparison to CO_2. This approach follows from the well-known dominance of the S_{cw} term in (13) for determining k for weakly soluble gases.

[14] Recently COAREG was extended to include the case of an atmospheric gas (such as ozone) that reacts strongly in the ocean [*Fairall et al.*, 2007]. Using the notation from *Fairall et al.* [2000], the budget equation for the oceanic concentration of a chemical, C_w, is

$$\partial C_w/\partial t + \vec{U}\cdot\nabla C_w = -\frac{\partial[-(D_c+K)\partial C_w/\partial z]}{\partial z} - aC_w, \quad (18)$$

where z is the vertical coordinate (depth for the ocean), D_c is the molecular diffusivity of C_w in water, K the turbulent eddy diffusivity, and the last term is the loss rate of C_w due to reactions with chemical Y. Thus, $a = Rcy\ Y$, where Y is the concentration of the reacting chemical and Rcy the reaction rate constant. Assuming that the concentration of Y is much larger than C_w so that it remains effectively constant and that a is sufficiently large that C_w is completely removed within the molecular sublayer, *Garland et al.* [1980] showed that the water-side resistance is

$$\frac{u_*}{r_w} = \sqrt{aD_c}. \quad (19)$$

Fairall et al. [2007] relaxed the requirement that the reaction was confined to the molecular sublayer and obtained a solution that allowed the ozone deposition velocity to depend on the oceanic turbulence

$$\frac{u_*}{r_w} = \sqrt{aD_c}\frac{K_1(\xi_0)}{K_0(\xi_0)}. \quad (20)$$

Here K_0 and K_1 are modified Bessel functions of order 0 and 1 and

$$\xi_0 = \frac{2}{ku_*}\sqrt{aD_c}. \quad (21)$$

When a is large, ξ_0 is large and the ratio K_1/K_0 = 1. Thus, we recover the *Garland et al.* [1980] solution given in (19) and C_w approaches 0 for $z > D_c/\kappa u_*$.

2.4. Generalization for Trace Gas Fluxes

[15] The basic expressions for the COAREG3.0 algorithm are formulated generally in terms of forcing variables, gas solubility, and gas diffusivity (Schmidt numbers), but current code implementations are gas specific (i.e., a MATLAB script for CO_2 and a separate script for DMS, etc). Recently, *Johnson* [2010] published a numerical scheme to calculate temperature- and salinity-dependent air-water transfer velocities for any gas. *Rowe et al.* [2011] implemented Johnson's method for a list of 79 trace gases; the chemical parameter, CP_c, is shown in Figure 1 for selected gases in

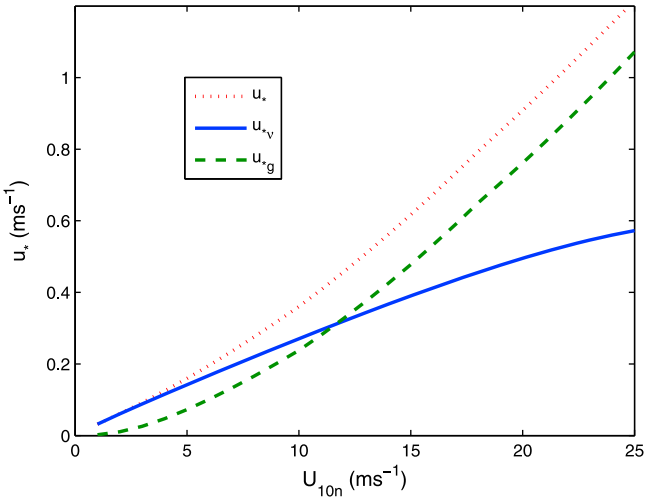

Figure 2. Friction velocity u_* as a function of 10 m neutral wind speed. The dotted line is the COARE3.0 standard Charnock specification for the total drag. The solid line is $u_{*\nu}$ from tangential (viscous) drag following *Mueller and Veron* [2009] assuming flow separation fraction is equal to whitecap fraction. The dashed line is u_{*g} from the wave drag computed as the difference between COARE3.0 and the tangential stress.

order of solubility. One can think of CP_c as the flux normalized by the forcing. CP_c varies over 4 orders of magnitude, leveling off at high solubility when the atmospheric transfer becomes the limiting process. For example, CO_2 is the 18th gas on the list, and $CP_c = 1.31\ 10^{-4}$; for these conditions $k = u_* CP_c/\alpha = 24.4$ cm h^{-1}.

[16] Note, Johnson's approach is meant to account for molecular size and polar interactions that are reflected in the Henry's constant for fresh water, but it does not account for hydration/dehydration reactions and acid-base equilibrium. Thus, it applies for neutral species in pure water only, and the apparent solubility will be higher for the 10 compounds in Figure 1 that undergo oxidation and/or hydrated/acid-base reactions (e.g., ozone or SO_2) under ambient conditions (especially in seawater where nonideal behavior of ions is greater).

3. Recent Advances in Bulk Flux Parameterizations

[17] In this section, we discuss new observations and theoretical issues associated with wave effects and the partition of total wind stress at the surface into tangential (viscous) and gravity wave (pressure) components in the context of molecular sublayer versus bubble-mediated transfer processes. The focus is on implications for simplified representations used in the current versions of the COARE parameterizations. As discussed in section 2.4, *Johnson* [2010] recently published a prescription to treat gas transfer parameters (solubility and Schmidt numbers) more generally. To estimate gas transfer velocity from bulk variables, the COAREG3.0 algorithms are applied sequentially: the bulk variables are passed to COARE3.0 which returns meteorological fluxes and scaling parameters; then a subset of bulk variables, fluxes, and u_* are passed to COAREG3.0.

[18] In section 2.2, we noted that COARE3.0 is a good fit to mean observed momentum and heat transfer coefficients over a considerable range of wind speeds (with more observations needed at $U_{10} > 18$ m s^{-1}). However, at any specific wind speed bin there is considerable scatter, more than can be explained by atmospheric sampling variability alone (in comparison to the scatter for a meteorological scalar flux such as evaporation). Also, the increasing influence of waves on the stress may be contained in the Charnock relation (5) with a fixed value of a_C, but COARE3.0 requires a *wind speed–dependent* Charncock parameter to fit the data. Thus, it is clear that over the open ocean there is, on average, a systematic change in the wind-wave balance with increasing wind speed. Attempts to find simple scaling expressions that explain variations in surface roughness length (or drag coefficient) due to variations in surface wave properties have been of limited success [*Drennan et al.*, 2005].

[19] For gas transfer there is a theoretical argument that the oceanic molecular sublayer physics should be dominated by the viscous part of the stress. This concept is developed in detail by *Soloviev and Lukas* [2006] and is implemented in the *Soloviev* [2007] gas transfer model. The idea can be simply summarized by noting that (5) represents the surface roughness as the sum of viscous and gravity wave parts [*Smith*, 1988]

$$z_o = z_{o\nu} + z_{og}, \tag{22}$$

but we can also similarly represent the stress

$$\tau = \tau_v + \tau_g. \tag{23}$$

The argument is that viscous stress directly drives the molecular/turbulent term in k_w, but the gravity wave stress should be used to scale the bubble term because it is associated with breaking waves. In Appendix A we illustrate how this applies in the COAREG3.0 algorithm. Crudely stated, we represent k as

$$k(1 + \alpha r_a/r_w) = \frac{u_{*\nu}}{r_{wt}} + k_b\left(u_{*g}\right). \tag{24}$$

Of course the difficulty is to specify the partition of the total stress into the two components and to determine the functional dependence of the bubble term on u_{*g}. For the partition aspect we have initially used the development from *Mueller and Veron* [2009]. See Appendix B for more detail on how this is done; also see *Yang et al.* [2011] for application to an analysis of k for DMS. COAREG3.0 does not distinguish between $u_{*\nu}$ and u_{*g}, total u_*, is used in the first term in (24) and a U_{10}-dependent whitecap equation is used in the second term. The significance for the first term on the RHS in (24) is illustrated in Figure 2, where total u_*, $u_{*\nu}$, and u_{*g} are shown as a function of wind speed using the stress partitioning in Figure B1. For wind speed between 2 and 10 m s^{-1}, $u_{*\nu}$ is almost linear. At $U_{10} = 10$ m s^{-1}, it is 28% less than total u_*, and it is 47% less at $U_{10} = 20$ m s^{-1}.

[20] There is considerable uncertainty in the correct partitioning of the stress. The *Mueller and Veron* [2009] approach gives quite different results compared to *Soloviev*'s [2007].

Table 2. Ocean Trace Gas Flux Observations by Covariance Methods

Gas	Designation	Reference
CO_2	Gasex98 and Methods[a]	*McGillis et al.* [2001a, 2001b]
	Gasex01[a]	*McGillis et al.* [2004]
	Methods	*Miller et al.* [2010]
	Methods	*Prytherch et al.* [2010]
	North Atlantic	*Lauvset et al.* [2011]
	SO GasEx[a]	*Edson et al.* [2011]
DMS	SE Pacific[a]	*Huebert et al.* [2004]
	North Atlantic and SE Pacific[a]	*Blomquist et al.* [2006]
	North Pacific[a]	*Marandino et al.* [2007]
	South Pacific[a]	*Marandino et al.* [2009]
	Methods[a]	*Blomquist et al.* [2010]
Ozone	Methods	*Bariteau et al.* [2010]
	Gulf of Mexico	*Grachev et al.* [2011]
	Five Regions[a]	Helmig et al. (submitted manuscript, 2011)

[a]Data used in this paper.

Furthermore, the use of (24) assumes that breaking waves do not contribute to the direct molecular transfer, whereas it is known that wave breaking enhances near-surface turbulence intensity, mixing, and dissipation. *Soloviev* [2007] deals with this by adding a whitecap-weighted contribution of wave dissipation to the molecular transfer coefficient. There are also questions about the proper representation of the breaking wave properties in the bubble term. The present U_{10}-dependent whitecap equation is empirical and the use of the adjustable parameter B allows us to "calibrate" the algorithm to observed gas fluxes. However, a more physically based approach would link bubble forcing directly to some property of breaking waves. *Long et al.* [2011] have scaled the production of bubble-mediated aerosols with the rate of entrainment of air into water (units m s^{-1}, the same as V_o in (16)) by wave breaking

$$F_{Ent} = Const. * \varepsilon_d, \tag{25}$$

where ε_d is the energy dissipated by wave breaking per unit area (Wm^{-2}). Thus, in principle the $V_o f_{wh}$ term in (16) for k_b could be replaced by F_{Ent}. If there is an approximate local balance of wave energy input and dissipation, then the wave breaking dissipation is approximately equal to the kinetic energy flux from the atmosphere into wave kinetic energy [*Terray et al.*, 1996]

$$\dot{E}_w = \rho_a u_{*g}^2 \langle C_p \rangle \cong \varepsilon_d, \tag{26}$$

where $\langle C_p \rangle$ is the mean wave momentum input weighted wave phase speed. However, this balance is only approximate as energy transfer via nonlinear wave-wave interaction can be significant in the equilibrium subrange [e.g., *Ardhuin et al.*, 2010].

[21] Given the difficulty of obtaining accurate global estimates of even U_{10} it is worthwhile to consider the added value of using more complex and less obtainable wave variables to characterize bubble-mediated gas exchange. Aside from the intellectual purity of using the actual physics instead of a linear regression, the existence of strong regional differences in wind-wave climatology are well established [*Hanley et al.*, 2010], methods to incorporate wave properties into global satellite gas transfer products are being developed [*Fangohr et al.*, 2008], and there are increased efforts to develop fully coupled atmosphere-wave-ocean prognostic climate models [*Witek et al.*, 2007].

[22] In the short-term, we are now implementing an update to the gas transfer algorithm, COAREG3.1, that incorporates the tangential stress concept discussed above. That requires a retuning of the A and B coefficients (see section 4). For the next version to replace COARE3.0, we are exploring the use of adding one simple wave parameter, wave age $W_a = C_p/U_{10}$, and using a state-of-the-art wind-wave model [e.g., *Banner and Morison*, 2010] to represent the effects on the drag coefficient. This will require a database of flux observations with coincident wave parameters. Stay tuned for future developments.

4. Synthesis of Recent Observations

[23] In this section, we examine data from several recent field programs. First, we summarize results comparing COARE3.0 with an ensemble of observations of meteorological fluxes from three research groups. Then, we attempt to rationalize the adjustable parameters in COAREG3.1 for CO_2 and DMS using observations from the three GasEx field programs plus published results from five other DMS field programs. The observations we use are (see Table 2) all based on the eddy covariance method, but observational details are not given here. Sonic anemometers, platform motion corrections, and infrared absorption fast humidity sensors were used by each group, but instruments and software were essentially independent.

4.1. Meteorological Flux

[24] Comparison with observations of meteorological fluxes is based on a compilation of flux data obtained from the ESRL series of cruises, the University of Connecticut (UConn) database (principally the Martha's Vineyard offshore platform and buoys deployed as part of the CLIMODE project), and the University of Miami (UMiami) spar buoy flux database. Each group provided the mean and standard deviation of the 10 m neutral transfer coefficient in wind speed bins from 1 to 24 m s^{-1}: ESRL, C_{d10n} and C_{E10n} (5290 values of averaging time T = 1 h between 2 and 19 m s^{-1}); UConn, C_{d10n} and C_{H10n} (14,900 30 min values between 2 and 24 m s^{-1}); UMiami, C_{d10n} (6500 30 min values between 3 and 17 m s^{-1}). The statistical uncertainty of a single observation of C_{d10n} (computed directly from the distribution of values within a wind speed bin) is approximately 0.4 10^{-3} for each database. The ship data are obtained at a height of 18 m above the surface while the other two data sets are nominally at a height of 5 m. Since the uncertainty in the flux [*Blomquist et al.*, 2010] scales approximately as $\sqrt{z/T}$, the larger random uncertainty associated with ship-based fluxes observed at greater height was approximately compensated by the longer averaging time. Flow distortion effects on the mean wind speed associated with the ship structure were corrected based on wind tunnel studies, numerical flow calculations, and comparisons with buoys [*Fairall et al.*, 1997; *Dupuis et al.*, 2003]. In Figure 3 we show final results for the transfer coefficient from each data set plus the mean of all three. The COARE3.0 values are found to agree very closely with the mean of the measurements for $U_{10n} < 19$ m s^{-1}: 5.5%

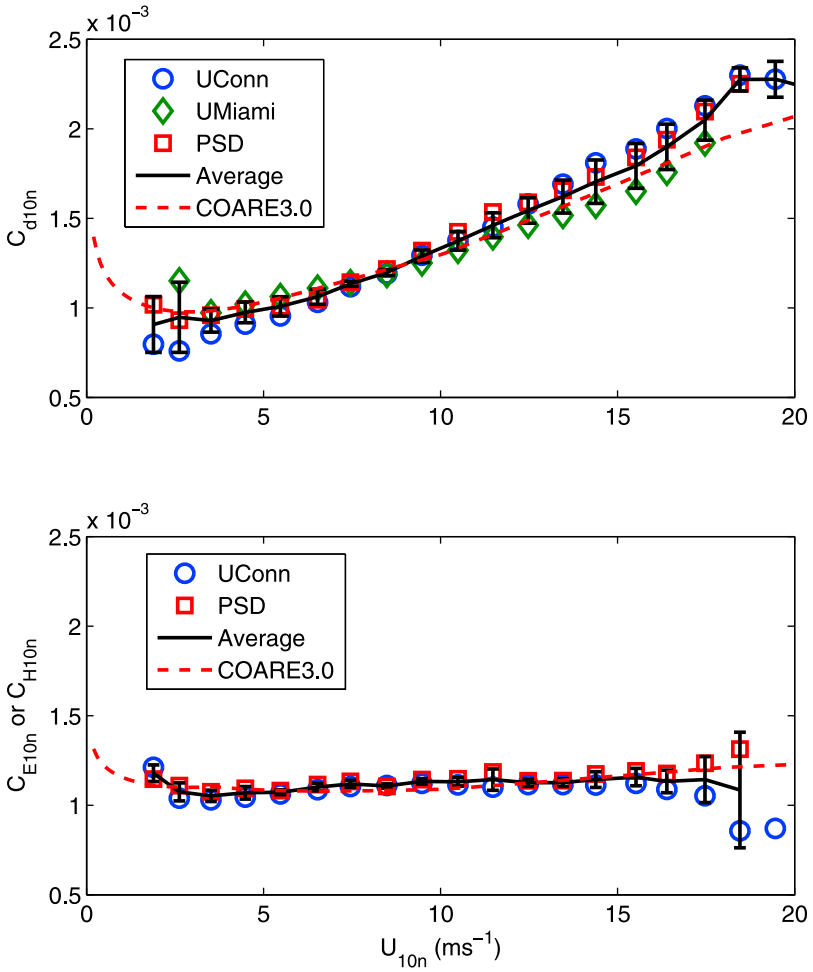

Figure 3. The 10 m neutral turbulent transfer coefficients as a function of 10 m neutral wind speed from direct surface-based observations. Symbols are as follows: circle, University of Connecticut (floating instrument platform, Martha's Vineyard Observatory, and moored buoys); diamond, University of Miami (Air-Sea Interaction Spar buoy); square, Physical Sciences Division NOAA ESRL (ships): (top) C_{d10n} and (bottom) C_{E10n} (ESRL/PSD) and C_{H10n} (University of Connecticut). The black line is the mean of the data sets; the error bars are statistical estimates of the uncertainty in the mean.

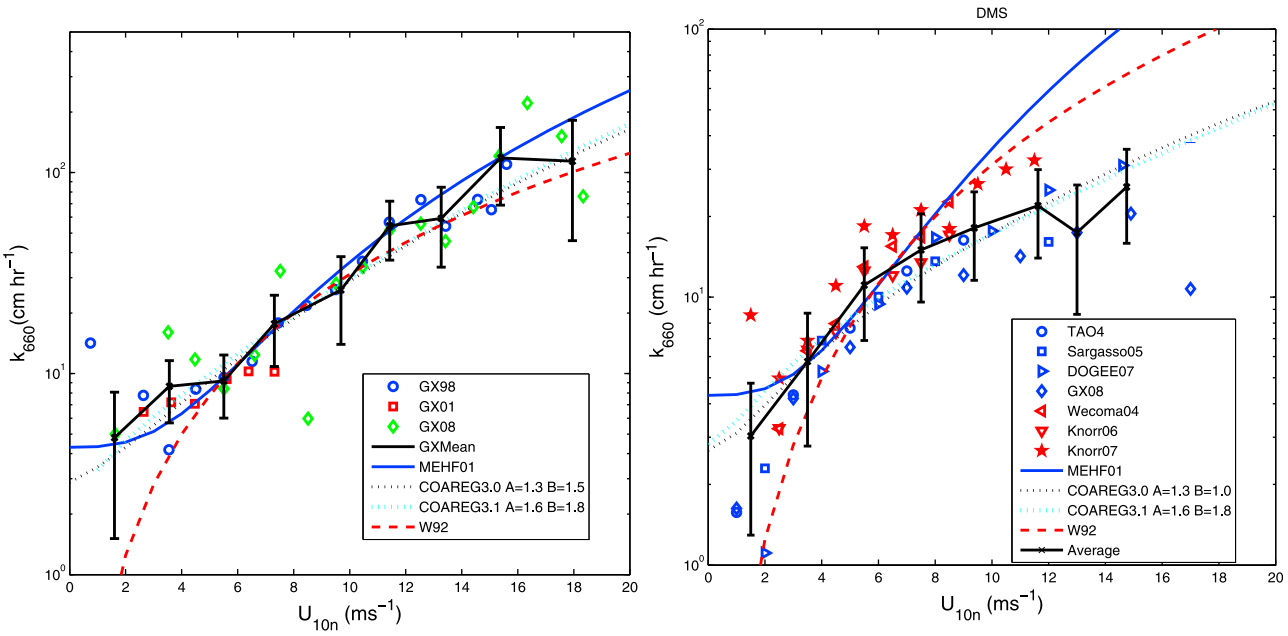

Figure 4. (left) Gas transfer coefficient for CO_2 as a function of 10 m neutral wind speed from direct surface-based observations. The black line is the mean of the data sets; the error bars are statistical estimates of the uncertainty in the mean computed as described in the text. Symbols are as follows: circles, GASEX98; squares, GASEX01; diamonds, SOGASEX08. The parameterizations shown are as follows: blue solid line, *McGillis et al.* [2001a]; black dotted line, COAREG3.0 CO_2; cyan dotted line, COAREG3.1 CO_2 using tangential u_*; red dashed line, W92. (right) DMS gas transfer coefficient as a function of 10 m neutral wind speed from direct surface-based observations. The black line is the mean of the data sets; the error bars are statistical estimates of the uncertainty in the mean computed as described in the text. Symbols are as follows: circles, TAO04 (equatorial Pacific); squares, Sargasso Sea 05; right triangles, DOGEE07; diamonds, SOGASEX08; left triangles, Wecoma04; inverted triangles, Knorr06; pentagrams, Knorr07. The parameterizations shown are as follows: blue solid line, *McGillis et al.* [2001a]; black dotted line, COAREG3.0 *DMS*; cyan dotted line, COAREG3.1 *DMS* using tangential u_*; red dashed line, W92.

for C_{d10n} and 4.2% C_{E10n} and C_{H10n}. Sensible heat and moisture coefficients are treated identically in COARE3.0 and this is verified for $U_{10n} < 19$ m s^{-1} in the observations.

4.2. CO_2 and DMS Flux

[25] A similar approach was followed for k values of CO_2 and DMS using all ship-based direct eddy covariance flux measurements. CO_2 k values from the first two GasEx field programs were combined with the mean estimates from Souther Ocean (SO) GasEx [*Edson et al.*, 2011; *Ho et al.*, 2011]. Rather than use the raw individual observations, the results shown here are based on processing the mean results from each field program provided in wind speed bins. GasEx 98 and GasEx 01 used closed path Licor 6262 fast response CO_2 sensors in temperature-controlled boxes; the results for SO GasEx were obtained using open path Licor7500 sensors. Despite efforts to keep salt and ship effluent from contaminating the open path optics, the SO GasEx CO_2 observations suffered from large humidity-CO_2 cross talk. Two methods were used to remove the humidity crosstalk [*Edson et al.*, 2011] and the final SO GasEx k values used here are the uncertainty-weighted average of the two. For DMS, observations from the University of California, Irvine (designated Wecoma04, Knorr06, and Knorr07) were combined with those from the University of Hawaii group (designated TAO04, Sargasso05, DOGEE07, and GX08). All fast response DMS data were obtained with APIMS isotopically labeled technology [*Marandino et al.*, 2007; *Blomquist et al.*, 2010]. For CO_2 there are 3,464 individual observations which yielded 41 values in wind speed bins from all three field programs; for DMS the corresponding numbers are 1192 and 38. The results are shown as a function of U_{10n} in Figure 4. To obtain the uncertainty in the mean estimates shown in Figure 4 we first computed the standard deviation of k within the ith wind speed bin, σ_{ki}; a mean normalized standard deviation ($\sigma_{kNorm} = \langle \sigma_k / k \rangle$) was computed. The final uncertainty in the mean value of k in the ith bin was estimated as $\sigma_{\langle k \rangle i} = [\sigma_i + \langle k \rangle_i \, \sigma_{kNorm}]/2/\sqrt{N_i - 1}$ where N_i is the number of values in the grand average wind speed bin (N_i varied from 2 to 7).

[26] The COARE algorithm group has been working from a gas transfer physics similarity hypothesis, if the physical formulation is reasonably complete then the empirical constants (e.g., A and B) should be the same for all gases. One way to examine this is to isolate one aspect of the physics. For example, to isolate the nonbubble part of the transfer we use (24) and the development in Appendix A, to write

$$\frac{\left[k_{660}\left(1+\frac{\alpha r_a}{r_w}\right) - k_{b660}\right]}{\phi u_{*\nu}} = 37.5A. \qquad (27)$$

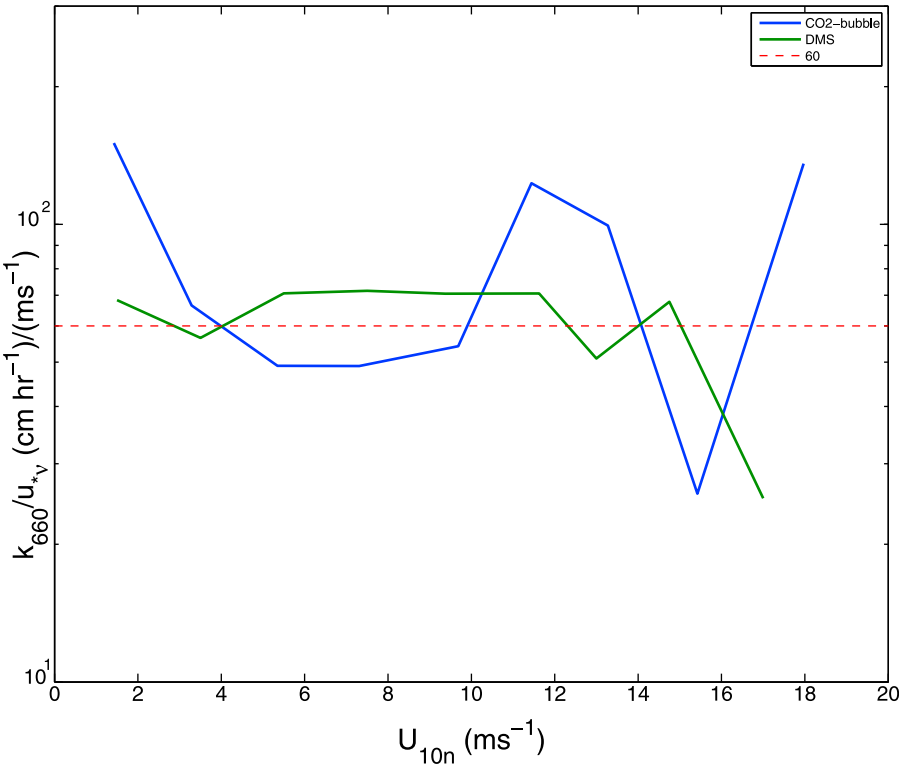

Figure 5. Analysis of the nonbubble transfer coefficient for CO_2 and DMS using (27) and the combined averages computed in section 4. The dashed line in the figure corresponds to 37.5 A = 60.

To apply (27), we must "bootstrap" the process since all variables on the LHS of (27) were not measured independently. We use COAREG3.0 for r_a/r_w (A14) and the Woolf model for k_{b660} with the average values of k_{660} taken from Figure 4. The results for both CO_2 and DMS are shown in Figure 5; the best fit to both gases is A = 60/37.5 = 1.6.

[27] One interesting aspect of this analysis is illustrated by returning to Figure 4. There are two versions of COAREG used here, the present version COAREG3.0 and a modified version, COAREF3.1, that uses $u_{*\nu}$ instead of u_* in the A term. While it is true that COAREG3.0 fits the data as well as COAREG3.1, the COAREG3.1 algorithm produces a good fit using the same values of A and B for both CO_2 and DMS.

4.3. Ozone Flux

[28] Because the ocean is essentially always a sink for ozone, the ozone flux is negative and the transfer velocity is conventionally referred to as a deposition velocity, V_d. Ozone enters the ocean from the atmosphere and is consumed by chemical reaction near the surface so that at depth the oceanic ozone concentration is zero. The flux is computed using only the atmospheric concentration

$$F_{Oz} = -\alpha_{Oz} k C_{aOz} = -V_d C_{aOz}. \tag{28}$$

The extension of COAREG to ozone was paralleled by the development of a ship-deployable fast response ozone sensor [*Bariteau et al.*, 2010]. The system has been deployed on five oceanic field programs (D. Helmig et al., Atmosphere-ocean ozone fluxes during the TexAQS 2006, STRATUS 2006, GOMECC 2007, GasEx 2008, and AMMA 2008 cruises, submitted to *Journal of Geophysical Research*, 2011). *Grachev et al.* [2011] analyzed observations from the Gulf of Mexico and found a good fit of COAREG3.0_ozone to ozone fluxes using a value $a = 10^3$ s^{-1} for the reactivity parameter. A more detailed evaluation of ozone flux results from the five research cruises is presented by Helmig et al. (submitted manuscript, 2011), but it is of sufficient interest to show representative work here. Figure 6 shows V_d as a function of U_{10n} for the five cruises. There is an obvious regional difference in the results of these field programs with the largest k values observed in the Gulf of Mexico and the smallest in the southern oceans (SO GasEx and the stratus region off Chile). These regional differences are roughly consistent with a global model assessment of ozone reactivity [*Ganzeveld et al.*, 2009, Figure 6]. Two field programs at intermediate latitudes show some agreement with the algorithm using $a = 10^2$ s^{-1}. According to the model physics, the lower the value of a, the stronger the wind speed dependence of k, because ocean turbulence plays an increasing role in the mixing. The average wind speed dependences shown in Figure 6 are not consistent with the model. This may be due to the fact that it is not reasonable to assume that a will necessarily be independent of wind speed. The algorithm is not consistent with details of the observations in the Southern Ocean results, where there are low values for k (assumed to be associated with low values of a) but essentially no wind speed dependence. Based on these observations, it appears that some fundamental assumption in the algorithm is not met in this region. For example, the assumption that the profile of the concentration of the (unspecified) agent reacting

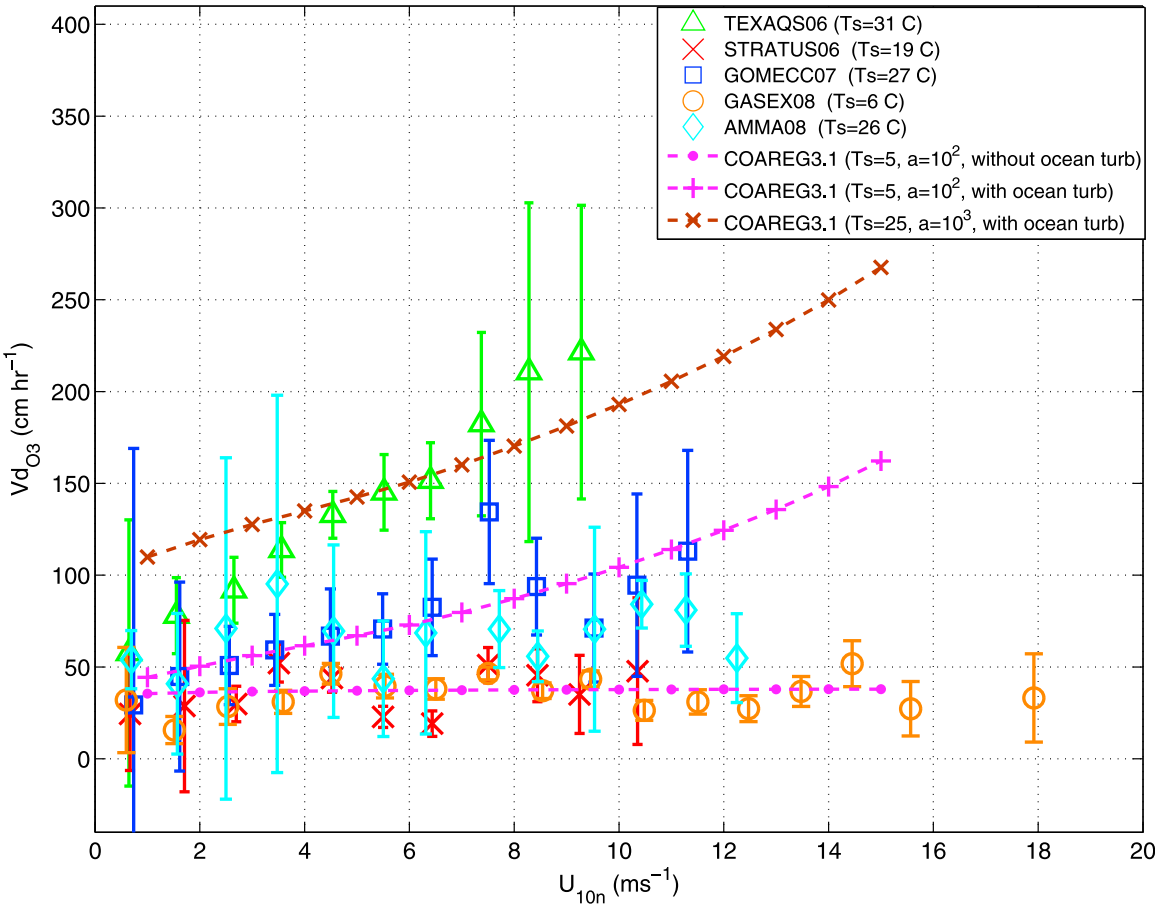

Figure 6. Wind speed bin-averaged ozone transfer velocities (symbols) for all deployments. The COAREG3.1 ozone model transfer velocities at different values of a are shown as dashed lines. T_s is sea surface temperature and a is reactivity.

with ozone in the water is constant and unaffected by ozone may be questioned. These findings illustrate that direct observations of ozone flux for parameterization purposes need to be supplemented with measurements of oceanic variables that relate to the water-side ozone chemistry.

5. Conclusion

[29] In this paper, we examine and discuss updates for the COARE physically based bulk flux algorithms. First, the current 3.0 versions are discussed and a generalization of the gas transfer codes to a much larger number (79) of gases is described. We describe new physics associated with wave effects and the partition of total wind stress at the surface into tangential (viscous) and gravity wave (pressure) components. Finally, both meteorological and gas transfer coefficients are tested against combined data sets from an ensemble of recent field programs.

[30] Wave information is needed to account for nonrandom variability in the relationship of surface roughness to the wind speed. COARE3.0 includes user-selectable scaling models of wave effects using wave age and wave height. Theoretically, viscous stress is more directly associated with the turbulent/molecular sublayer component of gas transfer while wave stress is associated with the bubble-mediated transfer. In section 3 and Appendices A and B, we show how this fits into

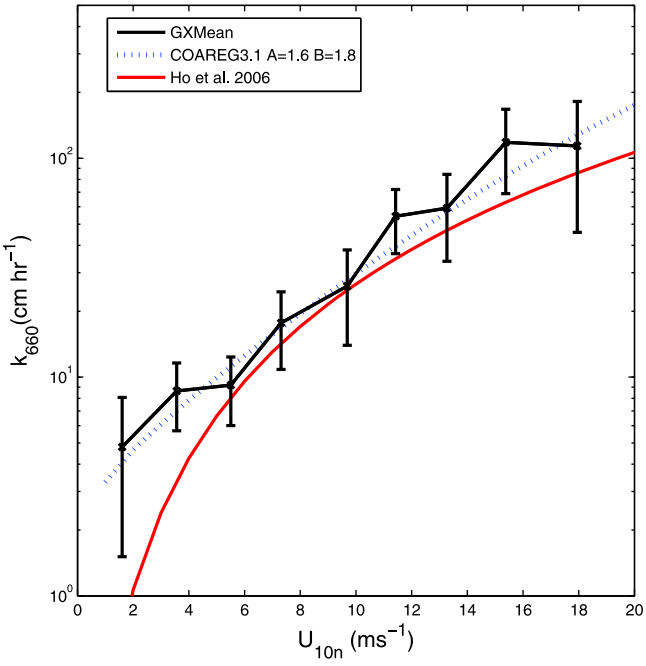

Figure 7. CO_2 gas transfer coefficient as a function of 10 m neutral wind speed from eddy covariance atmospheric (black line) and dual deliberate tracer (red line) observations.

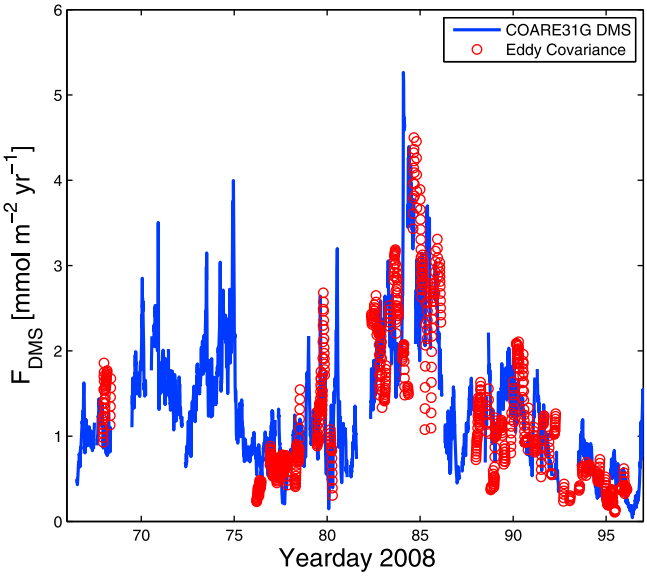

Figure 8. DMS flux time series from the SOGASEX08 field program: line, COAREG31DMS; circles, direct covariance observations that pass quality filters.

the COAREG physics structure by introducing the viscous friction velocity, $u_{*\nu}$, and the gravity wave friction velocity, u_{*g}. Lacking a flux and wave parameter database, we decided to delay a new version of the meteorological model and replacement of the whitecap scaling in the bubble-mediated term in COAREG. However, we implemented an update to the gas transfer algorithm (version COAREG3.1) that includes the partition of tangential and wave stress.

[31] The current meteorological version COARE3.0 was compared with a collection of nearly 26,700 observations of drag and heat transfer coefficients (compiled from numerous field programs of three independent research groups). The algorithm agreed overall within 5% with observations averaged in wind speed bins over a 10 m neutral wind speed range of 2 to 18 m s^{-1}. Above 18 m s^{-1}, the disagreement increases but sampling statistics are poor. Observations of gas transfer k for CO_2 and DMS were normalized to a fixed Schmidt number of 660 (equivalent to that for CO_2 at 20°C). Using an ensemble of gas flux observations from 6 research groups and 9 field programs; mean k_{660} values in 10 m neutral wind speed bins were computed. Schmidt number normalization only approximately removes temperature modulation of k for moderately soluble gases such as DMS (see Appendix A); this is explored in more detail by *Yang et al.* [2011]. A reasonable fit of the mean k_{660} versus U_{10n} values was obtained for both CO_2 and DMS with a version of COAREG3.1 using $u_{*\nu}$ in the nonbubble term with the turbulent/molecular coefficient $A = 1.6$ and the bubble-mediated coefficient $B = 1.8$. See *Edson et al.* [2011] for a more detailed evaluation of the wind speed dependence of k_{660} for CO_2 and *Yang et al.* [2011] for DMS.

[32] One point to ponder is the differences in atmospheric covariance estimates versus oceanic estimates from deliberate dual tracer measurements. The nominal mean curve for CO_2 derived from tracer data [*Ho et al.*, 2006] is compared to the atmospheric covariance GasEx synthesis in Figure 7. The tracer data fall in the wind speed range 5 to 16 m s^{-1}, so there is probably little significance to the disagreement at low wind speeds. Within the relevant wind speed range, the tracer values are nominally 20% lower than the covariance values; the original W92 formula is 10% lower than the covariance values. Based on the error bars in Figure 7, the grand average k dependence from the covariance data is constrained to about 13%, while *Ho et al.* [2006] state the uncertainty of their quadratic coefficient as 7%. Eddy correlation observations of ^{3}He and SF_6 fluxes and/or numerical ocean turbulent mixing models could be used to address this issue.

[33] A more detailed evaluation of ozone flux results from the five research cruises is presented by Helmig et al. (submitted manuscript, 2011), but a preview of that work was briefly discussed. Regional differences in deposition velocity observations are consistent with global model projections [*Ganzeveld et al.*, 2009], but the wind speed dependence of the algorithm is much stronger than observations from the S. Atlantic and S. Pacific. To date this is unexplained.

[34] New MATLAB codes for COAREG3.1 (see Table 1) incorporating tangential stress with coefficients tuned to the observations discussed here are available at ftp://ftp1.esrl.noaa.gov/users/cfairall/bulkalg/gasflux/COAREG31_vectorized/. These versions of the algorithm have been restructured so that COARE3.0 is incorporated into the code rather than called separately and all subroutines are also incorporated into a single function. This is a vectorized code that will accommodate a matrix of data (i.e., a time series or spatial grid). The ftp site includes a driver program and a matrix data sample. A sample diagram of the time series of DMS flux (bulk and covariance) from the driver code is shown in Figure 8.

[35] While Figure 8 suggests good correlation of fluxes for DMS, the error bars in Figure 4 suggest substantial work is needed. One major problem is the poor performance of fast CO_2 sensors, which limit field work to regions with very large air-sea differences in CO_2 concentration. Some clarity in scientific issues could also come from high-quality eddy covariance measurements of gases more soluble than DMS and less soluble than CO_2. There is considerable room for progress on bubble-mediated transfer through field, laboratory, and numerical modeling studies.

Appendix A: Asymptotic Expansion of COAREG Gas Transfer Form

[36] The COAREG algorithm gives a simple form for the transfer velocity

$$k = \frac{u_*}{r_w + \alpha r_a}. \tag{A1}$$

We can separate the oceanic and atmospheric components as follows:

$$k(1 + \alpha r_a/r_w) = \frac{u_*}{r_w} = \frac{u_*}{r_{wt}} + k_b. \tag{A2}$$

The oceanic components are the sum of direct turbulent/molecular diffusion and bubble-mediated terms. We use (A2) to compute k_{660}

$$\frac{k_{660}}{u_*}(1 + \alpha r_a/r_w) = \frac{k}{u_*}\left[\frac{S_{cw}}{660}\right]^{1/2}(1 + \alpha r_a/r_w)$$
$$= \left[\frac{S_{cw}}{660}\right]^{1/2}\frac{1}{r_{wt}} + \left[\frac{S_{cw}}{660}\right]^{1/2}\frac{k_b}{u_*}. \tag{A3}$$

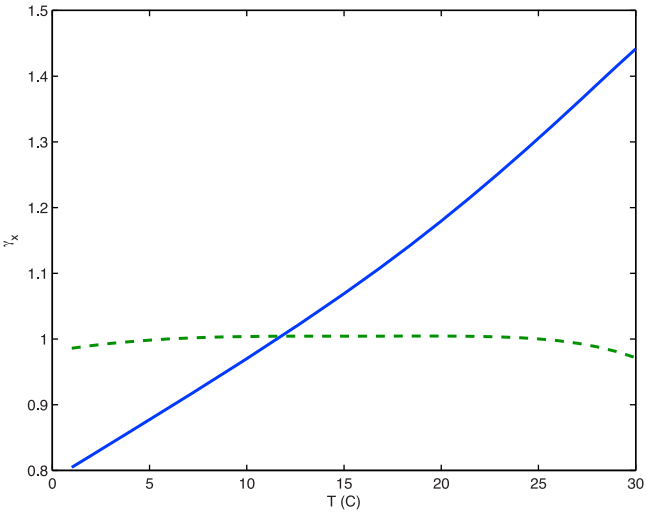

Figure A1. The Schmidt solubility factor as a function of temperature from (A8): dashed line, CO_2; solid line, DMS.

Using (13) the first term can be written

$$\left[\frac{S_{cw}}{660}\right]^{1/2}\frac{1}{r_{wt}} = (\rho_a/\rho_w)^{1/2}\left[h_w(660)^{1/2} + \left[\frac{S_{cw}}{660}\right]^{1/2}\kappa^{-1}\ln(z_w/\delta_w)\right]^{-1}. \tag{A4}$$

The molecular sublayer thickness in the ocean is on the order of 1 mm so for z_w~1 m, the second term in (A4) is about 5% of the first term. Neglecting the second term gives

$$\left[\frac{S_{cw}}{660}\right]^{1/2}\frac{1}{r_{wt}} \cong (\rho_a/\rho_w)^{1/2}\left[h_w(660)^{1/2}\right]^{-1} = (\rho_a/\rho_w)^{1/2}\frac{A\phi}{13.3(660)^{1/2}} = A\phi\Gamma. \tag{A5}$$

Except for light wind cases, $\phi = 1$ so $\Gamma = 1.04\ 10^{-4}$. There is a very weak temperature dependence of Γ through the density of air and because we neglected the log term in (A4).

[37] On the atmospheric side, the Schmidt numbers for most gases of interest are very near 1.0. Thus, we can use the transfer coefficient for water vapor, C_E, to estimate r_a to good accuracy. From *Fairall et al.* [2000], we can show that

$$r_a \cong C_d^{1/2}/C_E \cong 33. \tag{A6}$$

If we approximate $r_w^{-1} \cong \left[\frac{S_{cw}}{660}\right]^{-1/2} A\Gamma$, then (A3) becomes

$$\frac{k_{660}}{u_*}\left[1 + 3.3\times10^{-3}A\alpha(20)\gamma^{-1}\right] = A\Gamma\phi + \frac{k_{b660}}{u_*}, \tag{A7}$$

where

$$\gamma = \left[\frac{S_{cw}}{660}\right]^{1/2}\frac{\alpha(20)}{\alpha(T)}. \tag{A8}$$

For CO_2, the factor γ is close to 1.0 and essentially independent of temperature; for DMS, γ varies about a factor of 2 (see Figure A1). For DMS, the atmospheric resistance term is on the order of 5%; for CO_2 it is about 0.2%. Note (A6) implies r_a varies ±20% as wind speed varies from 0 to 20 m s^{-1}, so for more soluble gases this wind speed dependence may merit consideration.

[38] The low wind speed limit is affected by the buoyancy term, ϕ. From *Fairall et al.* [2000]

$$\phi(R_f) = \left(1 + R_f/R_{fc}\right)^{1/4}, \tag{A9}$$

where R_f is the oceanic turbulent Richardson number across the molecular sublayer and $R_{fc} = 1.5\ 10^{-5}$ is the critical value. The Richardson number can be expressed in terms of the surface fluxes as

$$R_f = \frac{g\rho_w\nu_w}{\rho_a c_{pw}}\frac{\left[\beta_T H_{tot} + \frac{\beta_S c_{pw}}{L_e}H_l\right]}{u_*^4}, \tag{A10}$$

where the β are the oceanic expansion coefficients for temperature (subscript T) and salinity (subscript S), H_{tot} and H_l are the total interfacial cooling rate (sum of sensible, latent, and net IR fluxes) and the latent heat, ν_w the kinematic viscosity of seawater, c_{pw} the specific heat, and L_e the latent heat of water. Substituting values for the physical constants (including the temperature dependence for β_T [*Fairall et al.*, 1996a]) yields

$$R_f/R_{fc} = 2.3\ 10^{-7}\left[(T+3.2)^{0.79}H_{tot} + 2.0H_l\right]/u_*^4, \tag{A11}$$

where T is in C. In the limit as wind speed approaches 0, only buoyancy flux contributes to gas transfer and (A10) and (A11) yield

$$u_*\phi(R_f) \to 0.021\left[(T+3.2)^{0.79}(H_s + H_l + R_{nl}) + 2.0H_l\right]^{1/4}, \tag{A12}$$

where R_{nl} is the net IR radiative flux at the surface. For the tropics, (A12) yields a nominal value of 0.13 while for high latitudes a typical value is 0.07 (with more variability than the tropics). This implies a zero wind speed transfer velocity, $A\Gamma u_*\phi$, of about 4.8 cm h^{-1} in the tropics and about 2.6 cm h^{-1} at high latitudes.

[39] The bubble driven part of the transfer is taken from *Woolf* [1997]

$$k_b = BV_o f_{wh}\alpha^{-1}\left[1 + \left(e\alpha S_{cw}^{-1/2}\right)^{-1/n}\right]^{-n}, \tag{A13}$$

where B is a second adjustable constant, V_o = 2450 cm h^{-1}, f_{wh} is the whitecap fraction, e = 14, and n = 1.2 for CO_2. The full COAREG3.0 expansion becomes

$$k\left[\frac{S_{cw}}{660}\right]^{1/2}\left(1 + 3.3\ 10^{-3}A\alpha(20)\gamma^{-1}\right) \cong 37.5A\left[1 + R_f/R_{fc}\right]^{1/4}u_* + \frac{BV_o f_{wh}}{\alpha(20)}\gamma G(T), \tag{A14}$$

where $G(T) = [1 + (e\alpha S_{cw}^{-1/2})^{-1/n}]^{-n}$. For relatively insoluble gases (defined as $e\alpha/S_c^{1/2} \ll 1$ or solubility much less than

about 2.0) the second term in $G(T)$ dominates while for relatively soluble gases $G(T) \rightarrow 1.0$. Thus

Insoluble

$$k_{b660} = \frac{BV_o e}{\sqrt{660}} f_{wh}, \text{ with } B = 1.0 \; k_{b660} \cong 1.33\,10^3 \, f_{wh} \quad \text{(A15a)}$$

Soluble

$$k_{b660} = \frac{BV_o \gamma(T)}{\alpha(20)} f_{wh}, \text{ with } B = 1.0 \; k_{b660} \cong \frac{2.4510^3 \gamma(T)}{\alpha(20)} \, f_{wh}. \quad \text{(A15b)}$$

For insoluble gases, k_{b660} has no temperature dependence. Note that CO_2 and DMS are both intermediate to these extremes, CO_2 is nearly "insoluble" and DMS is nearly "soluble." For DMS the factor multiplying f_{wh} is $0.18\ 10^3$ at $T = 20°C$ or about factor of 6 smaller than for CO_2.

[40] The COAREG3.0 algorithm uses a conventional specification of the whitecap fraction in terms of the 10 m neutral wind speed

$$f_{wh} = 3.84\,10^{-6} U_{10n}^{3.41}. \quad \text{(A16)}$$

As discussed in section 3, whitecap scaling is a surrogate for the direct production and mixing of bubbles. (A16) yields about 1% coverage (this formula describes so-called "stage B" whitecaps that includes the actively breaking region, stage A, plus the persistent bubble plume) at $U_{10n} = 10$ m s^{-1} and about 10% at $U_{10n} = 20$ m s^{-1}. This formula implies 100% whitecap coverage at a wind speed of about 39 m s^{-1}. Stage A whitecaps (the actively breaking region which is about 10% of the area of stage B) approximately obey such scaling to even higher wind speeds. However, the simple scaling used in (10) becomes questionable at very strong forcing when significant fractions of the bubbles may completely dissolve [*Woolf*, 1997; *McNeil and D'Asaro*, 2007].

[41] A u_*-based form for f_{wh} allows us to examine the balance of bubble and direct contributions in the context of tangential and wave stress (see Appendix B),

$$k\left[\frac{S_{cw}}{660}\right]^{1/2}\left[1 + \frac{3.310^{-3} A\alpha(20)}{\gamma}\right] \cong 37.5A\left[1 + R_f/R_{fc}\right]^{1/4} u_{*\nu} + \frac{BV_o \gamma G(T)}{\alpha(20)} f_{wh}\left(u_{*g}\right). \quad \text{(A17)}$$

The use of $u_{*\nu}$ rather than u_* causes the viscous term to be much more linear with wind speed while the use of u_{*g} causes the bubble term to be related to wave parameters. The R_f term causes k to have a nonzero value at low wind speeds with the zero intercept value dependent on the net nonsolar energy balance at the sea surface.

Appendix B: Tangential and Wave Stress Components

[42] The COARE3.0 algorithm follows *Smith* [1988] and assumes velocity roughness is represented as the sum of viscous (tangential shear) and gravity wave terms

$$z_o = a_C u_*^2/g + 0.11\nu/u_*, \quad \text{(B1)}$$

where values of the Charnock parameter, a_C, are obtained based on fits to mean drag coefficient data. If we specify a wind speed, then this equation can be used to compute u_* and the total drag coefficient

$$u_* = c_d^{1/2} U_{10} = \frac{\kappa}{\log(10/z_o)} U_{10n} \quad \text{(B2)}$$

by iterating between (B1) and (B2).

[43] *Mueller and Veron* [2009] approach the problem by assuming

$$\tau = \tau_v + \tau_g, \quad \text{(B3)}$$

where the subscript ν refers to the tangential stress and g refers to the wave stress (they actually split wave stress into form drag and breaking wave drag, but we will ignore that).

[44] *Mueller and Veron* [2009] define the tangential stress using the smooth flow roughness length

$$z_{o\upsilon} = 0.11\nu/u_{*\nu}, \quad \text{(B4)}$$

which gives the tangential drag coefficient

$$c_{d\nu}^{1/2} = \kappa/\log(10/z_{o\nu}). \quad \text{(B5)}$$

Thus, at a given wind speed one can iteratively compute the tangential stress using

$$u_{*\nu} = c_{d\nu}^{1/2} U_{10} = \frac{\kappa}{\log(10/z_{o\nu})} U_{10n}. \quad \text{(B6)}$$

For a given specification of U_{10n}, just cycle between (B4), (B5), and (B6) a few times and $u_{*\nu}$ is determined.

[45] The wave component is computed as a residual

$$u_{*g} = \left[u_*^2 - u_{*\nu}^2\right]^{1/2}. \quad \text{(B7)}$$

The wave component of the drag coefficient is

$$c_{dg}^{1/2} = u_{*g}/U_{10n} \quad \text{(B8)}$$

and the wave roughness length is $z_{og} = 10\exp\left[-\kappa/c_{dg}^{1/2}\right]$.

[46] When formulated in this manner, the tangential stress is independent of specification of wave properties so it is just a function of 10 m neutral wind speed. It can be approximated it as

$$c_{d\nu} = (0.9 - 0.4U_{10n}/25) * 10^{-3} \quad \text{(B9)}$$

for wind speed less than 30 m s^{-1}. Thus, the correction to the molecular component of the gas transfer velocity is just

$$u_{*\nu} = u_* \sqrt{c_{d\nu}/c_d}. \quad \text{(B10)}$$

One minor complication: *Mueller and Veron* [2009] actually allow for loss of tangential stress in regions of the surface with flow separation

$$\tau = \tau_v\left(1 - f_{sep}\right) + \tau_g, \quad \text{(B11)}$$

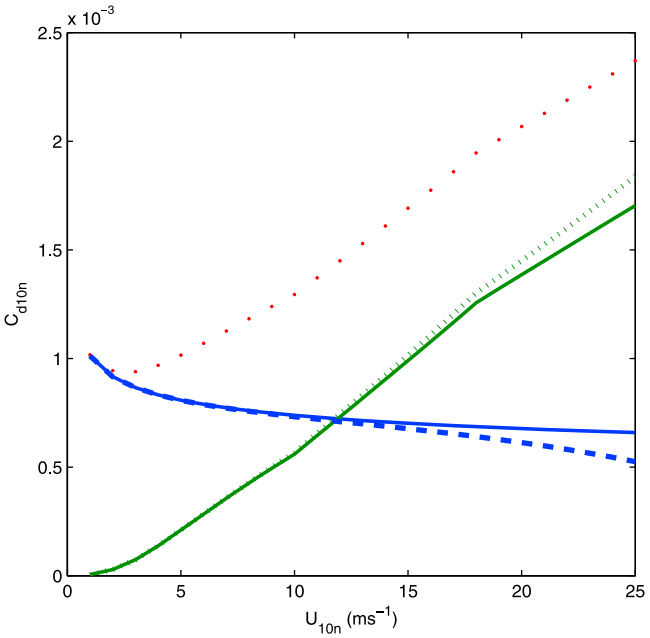

Figure B1. The 10 m neutral drag coefficient as a function of 10 m neutral wind speed. The red dots are the COARE3.0 specification for the total drag. The blue line is tangential drag that follows from (B4) and (B5). The green line is the wave drag computed as the difference between COARE3.0 and the tangential drag. The solid lines are computed with $f_{sep} = 0$ in (B11); the dashed lines are computed with $f_{sep} = 3.8\ 10^{-6} * U_{10}^{3.4}$.

where f_{sep} is the fractional area of the ocean surface exposed to airflow separation. They do not give results for f_{sep}, but if one assumes $f_{sep} = f_{wh}$ is the whitecap fraction, then the reduction is depicted in Figure B1.

[47] **Acknowledgments.** We thank the National Oceanic and Atmospheric Administration for the primary support of this work through grant NA07OAR4310084 and the National Science Foundation for additional support through grants ATM-0241611, ATM-0526341, OCE-0647475, and OCE-0424536. We also acknowledge support from NOAA CPO project GC07–186 and NOAA's Health of the Atmosphere program. We gratefully acknowledge Will Drennan and Eric Saltzmann for supplying data and Mark Rowe for producing Figure 1.

References

Ardhuin, F., et al. (2010), Semiempirical dissipation source functions for ocean waves. Part I: Definition, calibration, and validation, *J. Phys. Oceanogr.*, *40*, 1917–1941, doi:10.1175/2010JPO4324.1.

Banner, M. L., and R. P. Morison (2010), Refined source terms in wind wave models with explicit wave breaking prediction. Part I: Model framework and validation against field data, *Ocean Modell.*, *33*, 177–189, doi:10.1016/j.ocemod.2010.01.002.

Bariteau, L., J. Hueber, K. Lang, D. Helmig, C. W. Fairall, and J. E. Hare (2010), Ozone deposition velocity by ship-based eddy correlation flux measurements, *Atmos. Meas. Tech.*, *3*, 441–455, doi:10.5194/amt-3-441-2010.

Blomquist, B. W., C. W. Fairall, B. Huebert, and D. J. Kleiber (2006), DMS sea-air transfer velocity: Direct measurements by eddy covariance and parameterization based on the NOAA/COARE gas transfer model, *Geophys. Res. Lett.*, *33*, L07601, doi:10.1029/2006GL025735.

Blomquist, B. W., B. J. Huebert, C. W. Fairall, and I. C. Faloona (2010), Determining the sea-air flux of dimethylsulfide by eddy correlation using mass spectrometry, *Atmos. Meas. Tech.*, *3*, 1–20, doi:10.5194/amt-3-1-2010.

DeCosmo, J., K. B. Katsaros, S. D. Smith, R. J. Anderson, W. A. Oost, K. Bumke, and H. Chadwick (1996), Air-sea exchange of water vapor and sensible heat: The Humidity Exchange Over the Sea (HEXOS) results, *J. Geophys. Res.*, *101*, 12,001–12,016, doi:10.1029/95JC03796.

Drennan, W. M., P. K. Taylor, and M. J. Yelland (2005), Parameterizing the sea surface roughness, *J. Phys. Oceanogr.*, *35*, 835–848, doi:10.1175/JPO2704.1.

Dupuis, H., C. Guerin, D. Hauser, A. Weill, P. Nacass, W. M. Drennan, S. Cloché, and H. C. Graber (2003), Impact of flow distortion corrections on turbulent fluxes estimated by the inertial dissipation method during the FETCH experiment on R/V *L'Atalante*, *J. Geophys. Res.*, *108*(C3), 8064, doi:10.1029/2001JC001075.

Edson, J. B., C. W. Fairall, L. Bariteau, C. J. Zappa, A. Cifuentes-Lorenzen, W. R. McGillis, S. Pezoa, J. E. Hare, and D. Helmig (2011), Direct covariance measurement of CO_2 gas transfer velocity during the 2008 Southern Ocean Gas Exchange Experiment (SO GasEx): Wind speed dependency, *J. Geophys. Res.*, doi:10.1029/2011JC007022, in press.

Fairall, C. W., E. F. Bradley, J. S. Godfrey, G. A. Wick, J. B. Edson, and G. S. Young (1996a), The cool skin and the warm layer in bulk flux calculations, *J. Geophys. Res.*, *101*, 1295–1308, doi:10.1029/95JC03190.

Fairall, C. W., E. F. Bradley, D. P. Rogers, J. B. Edson, and G. S. Young (1996b), Bulk parameterization of air-sea fluxes for TOGA COARE, *J. Geophys. Res.*, *101*, 3747–3764, doi:10.1029/95JC03205.

Fairall, C. W., A. B. White, J. B. Edson, and J. E. Hare (1997), Integrated shipboard measurements of the marine boundary layer, *J. Atmos. Oceanic Technol.*, *14*, 338–359, doi:10.1175/1520-0426(1997)014<0338:ISMOTM>2.0.CO;2.

Fairall, C. W., J. E. Hare, J. B. Edson, and W. McGillis (2000), Parameterization and micrometeorological measurements of air-sea gas transfer, *Boundary Layer Meteorol.*, *96*, 63–106, doi:10.1023/A:1002662826020.

Fairall, C. W., E. F. Bradley, J. E. Hare, A. A. Grachev, and J. B. Edson (2003), Bulk parameterization of air-sea fluxes: Updates and verification for the COARE algorithm, *J. Clim.*, *16*, 571–591, doi:10.1175/1520-0442(2003)016<0571:BPOASF>2.0.CO;2.

Fairall, C. W., J. E. Hare, D. Helmig, and L. Ganzveld (2007), Water-side turbulence enhancement of ozone deposition to the ocean, *Atmos. Chem. Phys.*, *7*, 443–451, doi:10.5194/acp-7-443-2007.

Fairall, C., et al. (2010), Observations to quantify air-sea fluxes and their role in climate variability and predictability, in *Proceedings of OceanObs'09: Sustained Ocean Observations and Information for Society*, vol. 2, edited by J. Hall, D. E. Harrison, and D. Stammer, 13 pp., Eur. Space Agency, Paris.

Fangohr, S., D. K. Woolf, C. D. Jeffery, and I. S. Robinson (2008), Calculating long-term global air-sea flux of carbon dioxide using scatterometer, passive microwave, and model reanalysis wind data, *J. Geophys. Res.*, *113*, C09032, doi:10.1029/2005JC003376.

Ganzeveld, L., D. Helmig, C. Fairall, J. E. Hare, and A. Pozzer (2009), Atmosphere-ocean ozone exchange: A global modeling study of biogeochemical, atmospheric and water-side turbulence dependencies, *Global Biogeochem. Cycles*, *23*, GB4021, doi:10.1029/2008GB003301.

Garland, J. A., A. W. Etzerman, and S. A. Penkett (1980), The mechanism for dry deposition of ozone to seawater surfaces, *J. Geophys. Res.*, *85*, 7488–7492, doi:10.1029/JC085iC12p07488.

Grachev, A. A., L. Bariteau, C. W. Fairall, J. E. Hare, D. Helmig, J. Hueber, and E. K. Lang (2011), Turbulent fluxes and transfer of trace gases from ship-based measurements during TexAQS 2006, *J. Geophys. Res.*, *116*, D13110, doi:10.1029/2010JD015502.

Hanley, K. E., S. E. Belcher, and P. P. Sullivan (2010), A global climatology of wind–wave interaction, *J. Phys. Oceanogr.*, *40*, 1263–1282, doi:10.1175/2010JPO4377.1.

Hare, J., C. Fairall, W. McGillis, J. Edson, B. Ward, and R. Wanninkhof (2004), Evaluation of the National Oceanic and Atmospheric Administration/Coupled-Ocean Atmospheric Response Experiment (NOAA/COARE) air-sea gas transfer parameterization using GasEx data, *J. Geophys. Res.*, *109*, C08S11, doi:10.1029/2003JC001831.

Ho, D. T., C. S. Law, M. J. Smith, P. Schlosser, M. Harvey, and P. Hill (2006), Measurements of air-sea gas exchange at high wind speeds in the Southern Ocean: Implications for global parameterizations, *Geophys. Res. Lett.*, *33*, L16611, doi:10.1029/2006GL026817.

Ho, D. T., C. Sabine, D. Hebert, D. S. Ullman, R. Wanninkhof, R. C. Hamme, P. G. Strutton, B. Hales, J. B. Edson, and B. R. Hargreaves (2011), Southern Ocean Gas Exchange Experiment: Setting the stage, *J. Geophys. Res.*, C00F08, doi:10.1029/2010JC006852.

Huebert, B., B. Blomquist, J. E. Hare, C. W. Fairall, T. Bates, and J. Johnson (2004), Measurements of the sea-air DMS flux and transfer velocity using eddy correlation, *Geophys. Res. Lett.*, *31*, L23113, doi:10.1029/2004GL021567.

Johnson, M. T. (2010), A numerical scheme to calculate temperature and salinity dependent air-water transfer velocities for any gas, *Ocean Sci.*, *6*, 913–932, doi:10.5194/os-6-913-2010.

Lauvset, S. K., W. R. McGillis, L. Bariteau, C. W. Fairall, T. Johannessen, A. Olsen, and C. J. Zappa (2011), Direct measurements of CO_2 flux in the Greenland Sea, *Geophys. Res. Lett.*, *38*, L12603, doi:10.1029/2011GL047722.

Liss, P. S., and L. Merlivat (1986), Air-sea gas exchange rates: Introduction and synthesis, in *The Role of Air-Sea Interactions in Geochemical Cycling*, edited by P. Buat-Menard, pp. 113–129, D. Reidel, Hingham, Mass.

Long, M. S., W. C. Keene, D. J. Kieber, D. J. Erickson, and H. Marin (2011), A sea-state based source function for size- and composition-resolved marine aerosol production, *Atmos. Chem. Phys.*, *11*, 1203–1216, doi:10.5194/acp-11-1203-2011.

Marandino, C. A., W. J. De Bruyn, S. D. Miller, and E. S. Saltzman (2007), Eddy correlation measurements of the air/sea flux of dimethylsulfide over the North Pacific Ocean, *J. Geophys. Res.*, *112*, D03301, doi:10.1029/2006JD007293.

Marandino, C., W. De Bruyn, S. Miller, and E. Saltzman (2009), Eddy correlation measurements of the air/sea flux of dimethylsulfide over the eastern Pacific Ocean, *Atmos. Chem. Phys.*, *9*, 345–356, doi:10.5194/acp-9-345-2009.

McGillis, W. R., J. B. Edson, J. E. Hare, and C. W. Fairall (2001a), Direct covariance air-sea CO_2 fluxes, *J. Geophys. Res.*, *106*, 16,729–16,745, doi:10.1029/2000JC000506.

McGillis, W. R., J. B. Edson, J. D. Ware, J. W. H. Dacey, J. E. Hare, C. W. Fairall, and R. Wanninkhof (2001b), Carbon dioxide flux techniques performed during GasWx-98, *Mar. Chem.*, *75*, 267–280, doi:10.1016/S0304-4203(01)00042-1.

McGillis, W. R., J. B. Edson, C. J. Zappa, E. Terray, J. E. Hare, C. W. Fairall, W. M. Drennan, and M. A. Donelan (2004), Air-sea CO_2 fluxes in the equatorial Pacific, *J. Geophys. Res.*, *109*, C08S02, doi:10.1029/2003JC002256.

McNeil, C. L., and E. A. D'Asaro (2007), Parameterization of air-sea gas exchange at extreme wind speeds, *J. Mar. Syst.*, *66*, 110–121, doi:10.1016/j.jmarsys.2006.05.013.

Miller, S. D., C. Marandino, and E. S. Saltzman (2010), Ship-based measurement of air-sea CO_2 exchange by eddy covariance, *J. Geophys. Res.*, *115*, D02304, doi:10.1029/2009JD012193.

Mueller, J., and F. Veron (2009), A nonlinear formulation of the bulk surface stress over the ocean through a simple feedback mechanism, *Boundary Layer Meteorol.*, *130*, 117–134, doi:10.1007/s10546-008-9334-6.

Nightingale, P. D., G. Malin, C. S. Law, A. J. Watson, P. S. Liss, M. J. Liddicoat, J. Boutin, and R. C. Upstill-Goddard (2000), In situ evaluation of air-sea gas exchange using novel conservative and volatile tracers, *Global Biogeochem. Cycles*, *14*, 373–387, doi:10.1029/1999GB900091.

Oost, W. A., G. J. Komen, C. M. J. Jacobs, and C. van Oort (2002), New evidence for a relation between wind stress and wave age from measurements during ASGAMAGE, *Boundary Layer Meteorol.*, *103*, 409–438, doi:10.1023/A:1014913624535.

Perlinger, J. A., and M. D. Rowe (2008), Atmospheric transport and air-water exchange of hexachlorobenzene in Lake Superior, *Organohalogen Compd.*, *70*, 598–601.

Price, J. F., R. A. Weller, and R. Pinkel (1986), Diurnal cycling: Observations and models of the upper ocean response to diurnal heating, cooling, and wind mixing, *J. Geophys. Res.*, *91*, 8411–8427, doi:10.1029/JC091iC07p08411.

Prytherch, J., M. J. Yelland, R. W. Pascal, B. I. Moat, I. Skjelvan, and C. C. Neill (2010), Direct measurements of the CO_2 flux over the ocean: Development of a novel method, *Geophys. Res. Lett.*, *37*, L03607, doi:10.1029/2009GL041482.

Rowe, M. D., C. W. Fairall, and J. A. Perlinger (2011), Chemical sensor resolution requirements for near-surface measurements of turbulent fluxes, *Atmos. Chem. Phys.*, *11*, 5263–5275, doi:10.5194/acp-11-5263-2011.

Signorini, S. R., and C. R. McClain (2009), Effect of uncertainties in climatologic wind, ocean pCO_2, and gas transfer algorithms on the estimate of global sea-air CO_2 flux, *Global Biogeochem. Cycles*, *23*, GB2025, doi:10.1029/2008GB003246.

Smith, S. D. (1988), Coefficients for sea surface wind stress, heat flux, and wind profiles as a function of wind speed and temperature, *J. Geophys. Res.*, *93*, 15,467–15,472, doi:10.1029/JC093iC12p15467.

Soloviev, A. V. (2007), Coupled renewal model of ocean viscous sublayer, thermal skin effect and interfacial gas transfer velocity, *J. Mar. Syst.*, *66*, 19–27, doi:10.1016/j.jmarsys.2006.03.024.

Soloviev, A. V., and R. Lukas (2006), *The Near-Surface Layer of the Ocean: Structure, Dynamics, and Applications*, 572 pp., Springer, New York.

Soloviev, A. V., and P. Schlüssel (1994), Parameterization of the cool skin of the ocean and of the air-ocean gas transfer on the basis of modeling surface renewal, *J. Phys. Oceanogr.*, *24*, 1339–1346, doi:10.1175/1520-0485(1994)024<1339:POTCSO>2.0.CO;2.

Taylor, P. K., and M. A. Yelland (2001), The dependence of sea surface roughness on the height and steepness of the waves, *J. Phys. Oceanogr.*, *31*, 572–590, doi:10.1175/1520-0485(2001)031<0572:TDOSSR>2.0.CO;2.

Terray, E. A., M. A. Donelan, Y. C. Agrawal, W. M. Drennan, K. K. Kahma, A. J. Williams, P. A. Hwang, and S. A. Kitaigorodskii (1996), Estimates of kinetic energy dissipation under breaking waves, *J. Phys. Oceanogr.*, *26*, 792–807, doi:10.1175/1520-0485(1996)026<0792:EOKEDU>2.0.CO;2.

Vlahos, P., and E. C. Monahan (2009), A generalized model for the air-sea transfer of dimethyl sulfide at high wind speeds, *Geophys. Res. Lett.*, *36*, L21605, doi:10.1029/2009GL040695.

Wanninkhof, R. (1992), Relationship between wind speed and gas exchange over the ocean, *J. Geophys. Res.*, *97*, 7373–7382, doi:10.1029/92JC00188.

Wanninkhof, R., W. E. Asher, D. T. Ho, C. Sweeney, and W. R. McGillis (2009), Advances in quantifying air-sea gas exchange and environmental forcing, *Annu. Rev. Mar. Sci.*, *1*, 213–244, doi:10.1146/annurev.marine.010908.163742.

Webster, P. J., and R. Lukas (1992), TOGA-COARE: The Coupled Ocean–Atmosphere Response Experiment, *Bull. Am. Meteorol. Soc.*, *73*, 1377–1416, doi:10.1175/1520-0477(1992)073<1377:TCTCOR>2.0.CO;2.

Witek, M. L., P. J. Flatau, J. Teixeira, and D. L. Westphal (2007), Coupling an ocean wave model with a global aerosol transport model: A sea salt aerosol parameterization perspective, *Geophys. Res. Lett.*, *34*, L14806, doi:10.1029/2007GL030106.

Woolf, D. K. (1993), Bubbles and the air-sea transfer velocity of gases, *Atmos. Ocean*, *31*, 517–540, doi:10.1080/07055900.1993.9649484.

Woolf, D. K. (1997), Bubbles and their role in gas exchange, in *The Sea Surface and Global Change*, edited by P. S. Liss and R. A. Duce, pp. 173–206, Cambridge Univ. Press, Cambridge, U. K., doi:10.1017/CBO9780511525025.007.

Yang, M., B. W. Blomquist, C. W. Fairall, S. D. Archer, and B. J. Huebert (2011), Effects of sea surface temperature and gas solubility on air-sea exchange of dimethylsulfide (DMS), *J. Geophys. Res.*, *116*, C00F05, doi:10.1029/2010JC006526.

L. Bariteau, Cooperative Institute for Research in Environmental Sciences, University of Colorado at Boulder, 325 Broadway, Boulder, CO 80309-0216, USA.

B. Blomquist, B. Huebert, and M. Yang, Department of Oceanography, University of Hawai'i at Mānoa, 1000 Pope Rd., Honolulu, HI 96822, USA.

J. B. Edson, Department of Marine Sciences, University of Connecticut, 1080 Shennecossett Rd., Groton, CT 06340, USA.

C. W. Fairall and S. Pezoa, NOAA Earth System Research Laboratory, 325 Broadway, Boulder, CO 80305, USA. (chris.fairall@noaa.gov)

J. E. Hare, Joint Institute for Marine and Atmospheric Research, University of Hawai'i at Mānoa, Honolulu, HI 96822, USA.

D. Helmig, Institute of Alpine and Arctic Research, University of Colorado at Boulder, 1560 30th St., Boulder, CO 80309, USA.

W. McGillis, Lamont-Doherty Earth Observatory, Columbia University, 61 Route 9W, Palisades, NY 10964, USA.